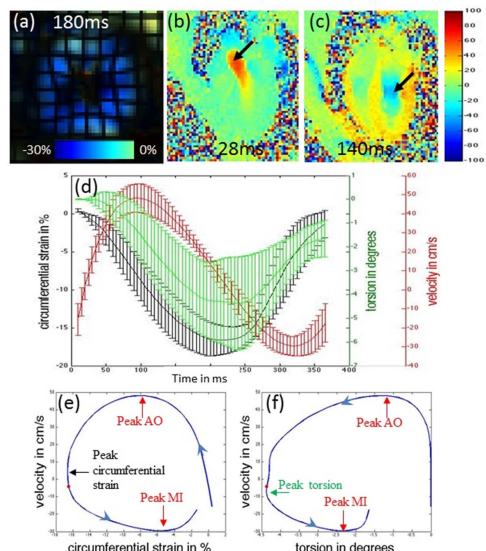


# Characterization of Cardiac Function in Naïve Non-Human Primates Using Strain and Flow Based MRI Biomarkers: A Test-Retest Reproducibility and Inter-Animal Variability Study

Smita Sampath<sup>1</sup>, Michael Klimas<sup>2</sup>, Richard Baumgartner<sup>3</sup>, Dai Feng<sup>3</sup>, Elaine Manigbas<sup>4</sup>, Ai-Leng Liang<sup>1</sup>, Brian Henry<sup>1</sup>, Jeffrey L Evelhoch<sup>2</sup>, and Chih-Liang Chin<sup>1</sup>

<sup>1</sup>Translational Medicine Research Center, Merck Sharp and Dohme, Singapore, Singapore, Singapore, <sup>2</sup>Imaging, Merck & Co. Inc., West Point, Pennsylvania, United States, <sup>3</sup>Biometric Research, Biostatistics and Research Decision Sciences, Merck & Co. Inc., Rahway, New Jersey, United States, <sup>4</sup>Imaging, Maccine Pte. Ltd., Singapore, Singapore

**Target Audience:** Researchers involved in non-human primate (NHP) basic research, drug discovery research, and pre-clinical animal model development, related to cardiovascular and metabolic disease.



**Figure 1** NHP Cardiac Function Characterization.

Representative end-systolic (a) circumferential strain (CS) and velocity maps depicting (b) aortic outflow, and (c) mitral inflow. (d) Time-curves for LV torsion, LV CS and composite velocity. Solid lines-mean, error bars-SD. Temporal inter-relationships are depicted in the partial loops (e) CS vs velocity & (f) torsion vs velocity.

**Table 1.** Intra-subject reproducibility (CCC analysis) for strain and flow based biomarkers measured in the NHPs.

Intra-Subject Reproducibility Statistics (cohort of 8 NHP)				
	Peak CS (%)	Systolic LSR (%)	Diastolic LSR (%)	Time to peak CS (ms)
Linear Regression (slope/R)	0.89/0.82	0.94/0.88	0.74/0.76	0.68/0.76
Bland Altman (mean diff/1.96*SD)	0.13/4.02	0.11/20.51	-1.64/42.37	-2.4/32.9
CCC_apical/[bound,abound]	0.75/[0.3,0.9]	0.97/[0.86,0.99]	0.92/[0.7,0.98]	0.94/[0.77,0.99]
CCC_mid/[bound,abound]	0.89/[0.6,0.97]	0.97/[0.87,0.99]	0.86/[0.51,0.97]	0.95/[0.8,0.99]
CCC_basal/[bound,abound]	0.87/[0.5,0.97]	0.89/[0.58,0.97]	0.87/[0.51,0.97]	0.83/[0.42,0.96]
	Peak LS (%)	Systolic LSR (%)	Diastolic LSR (%)	Time to peak LS (ms)
Linear Regression (slope/R)	0.77/0.75	0.71/0.72	0.90/0.72	0.80/0.74
Bland Altman (mean diff/1.96*SD)	0.16/4.93	-0.64/18.52	-3.11/46.28	-4.21/44.43
CCC_apical/[bound,abound]	0.88/[0.6,0.97]	0.7/[0.3,0.92]	0.84/[0.46,0.96]	0.81/[0.36,0.95]
CCC_mid/[bound,abound]	0.73/[0.2,0.93]	0.83/[0.6,0.97]	0.83/[0.41,0.96]	0.85/[0.48,0.96]
CCC_basal/[bound,abound]	0.9/[0.6,0.98]	0.89/[0.6,0.97]	0.84/[0.44,0.96]	0.9/[0.63,0.98]
	Peak mitral inflow (cm/s)	Peak aortic outflow (cm/s)	Time to peak aortic flow (ms)	Tps-pm (ms)
Linear Regression (slope/R)	0.85/0.77	0.83/0.61	0.95/0.7	0.79/0.92
Bland Altman (mean diff/1.96*SD)	2.02/8.04	3.62/14.77	15.38/8.4	3.75/14.58
CCC/[bound,abound]	0.75/[0.2,0.9]	0.57/[-0.06,0.88]	0.57/[0.54,0.59]	0.91/[0.65,0.98]

**Table 2.** Inter-subject reproducibility within the NHP cohort. (mean, SD, RSD, minimum sample size calculations).

Inter-Subject Variability Statistics (cohort of 8 NHP)				
(mean±SD) / RSD/minimum sample size	Peak CS (%)	Systolic LSR (%)	Diastolic LSR (%)	Time to peak CS (ms)
Apical	(-19.1±2.68) /14/8	(-97.30±20.07) /20/17	(115.34±24.10) /20/18	(235.94±28.26) /11/6
Mid	(-18.97±2.86) /15/9	(-97.20±19.09) /19/16	(114.70±23.02) /20/16	(234.79±24.68) /11/5
Basal	(-15.24±2.79) /18/14	(-73.24±19.21) /26/20	(86.76±30.92) /35/50	(231.09±26.53) /11/6
	Peak LS (%)	Systolic LSR (%)	Diastolic LSR (%)	Time to peak LS (ms)
Apical	(-14.66±3.42) /24/22	(-57.45±11.36) /20/16	(93.38±32.39) /34/48	(242.65±31.24) /13/7
Mid	(-14.88±2.56) /16/12	(-59.22±9.96) /17/12	(100.02±24.36) /24/24	(242.11±29.32) /12/6
Basal	(-15.66±2.83) /18/13	(-62.23±10.42) /16/12	(86.37±22.84) /26/28	(239.84±26.80) /11/5
	Peak mitral inflow (cm/s)	Peak aortic outflow (cm/s)	Tpa (ms)	Tps-pm (ms)
	(-31.07±2.36) /7/3	(48.89±4.39) /9/4	(165±20.87) /12.6/7	(85.05±4.41) /5/2

The evaluated functional biomarkers may provide imaging phenotypes in NHP models of cardiac disease and afford translatable non-invasive early markers of cardiac remodeling for preclinical longitudinal investigation of therapeutic responses.

**References:** [1] Narayanan et. al., Circ.: Cardiovasc. Imaging, 2:382-390, 2009. [2] Poirier et. al., Diabetes Care, 24: 5-10, 2001 [3] Axel et. al., Radiology, 172: 349-350, 1989. [4] Osman et. al., PMB, 45:1665-1682, 2000. [5] Brotman et. al., MRM, 69: 1421-1429, 2013. [6] Sampath et. al., JMIR, 27:809-817, 2008.

**Purpose:** Translational pre-clinical disease models offer a unique framework to evaluate novel therapeutics for human diseases. Specifically, NHPs are increasingly becoming an important non-rodent species selected for pre-clinical drug discovery and evaluation due to their phylogenetic similarity to humans. In particular, the identification of robust non-invasive functional imaging biomarkers for sensitive early assessment of NHP cardiac remodeling are critical to reducing overall costs involved in NHP model development and drug safety/efficacy research related to cardiac disease, and is currently grossly lacking in the literature. Herein, we present a study that employs the gold-standard magnetic resonance (MR) tagging method combined with phase-contrast (PC) imaging, both optimized for NHP imaging on a 3T MR imaging scanner to study systolic and diastolic function in NHP hearts through the quantitation of regional cardiac mechanics and intra-cardiac flow. We also present intra-subject reproducibility, inter-subject variability and power analyses in previously established strain and flow based biomarkers of early cardiac remodeling, known to precede LV volume changes and ejection fraction<sup>1,2</sup>. These biomarkers could serve in drug safety/efficacy/pharmacodynamic studies of experimental compounds in NHP cardiac models.

**Methods: Animals and Equipment:** Eight naïve Vietnamese cynomolgus macaques (weight: 3.6±0.2 kg (mean±SD)), age: 6±0 years, sex: 7 female, 1 male, anesthetized resting heart rate: 131±17 bpm were imaged using the 3T Trio MR imaging scanner (Siemens Medical Solutions, Erlangen, Germany) housed at Maccine's facility (Maccine Pte Ltd., Singapore). **Cardiac Functional MRI:** SPAMM<sup>3</sup> tagging (FOV: 150mm×150mm, imaging matrix: 208×208, slice thickness: 4mm, segments: 3, echo spacing: 7.3 ms, bandwidth: ±45KHz, TR/TE: 21.78 ms/3.39 ms, flip angle: 12°, tag separation: 4 mm) was employed to encode 2-D displacement in 3 short-axis (SA) slices and 2 long-axis (LA) slices. PC MR imaging (imaging parameters were identical to SPAMM tagging, except for TR/TE: 14.25 ms/4.49 ms, VENC: 100cm/s) was used to encode the chamber blood velocity in 2 LA planes with the mitral valve and aortic outflow tract in view respectively.

**Data Analysis:** All data analyses were conducted using in-house MATLAB programs. HARP4<sup>2</sup> image analysis methods were used to quantify regional myocardial displacement from the tagged images. Regional strain and torsion were then computed, and strain-based biomarkers were quantified: peak circumferential and longitudinal strain, time-to-peak strain, systolic and diastolic strain-rates, peak torsion, and torsion-rates. The average velocity around regions of interest near the mitral valve and the aortic valve were computed from the PC MRI datasets, and flow-based biomarkers were quantified: peak aortic outflow velocity, peak mitral inflow velocity, and time to peak velocity. An early diastolic combined strain-flow biomarker: time from peak strain to peak mitral inflow velocity ( $T_{ps-pm}$ ) was also quantified. All animals were imaged twice to obtain test and retest datasets. Statistical analyses were conducted to evaluate intra-subject reproducibility through concordance correlation coefficient (CCC) analysis. Inter-subject mean, standard deviation (SD) and relative standard deviations (RSD) were also calculated within the imaged cohort. Finally, prospective power analysis was conducted to estimate the minimum sample size needed to achieve 80% power for a 20% change at a  $P<0.05$  level using a two-tailed t-test.

**Results and Discussion:** NHP cardiac function closely resembles published results observed in humans<sup>5,6</sup> (Fig. 1). **Systole.** Circumferential and longitudinal LV shortening initiates early systolic pumping until peak aortic outflow (48.9±4.4 cm/s (mean±SD)) is achieved (Fig. 1e). Base-apex torsion (peak torsion of -4.4±1.9 degrees) dominates late pumping (Fig. 1f). Peak circumferential shortening during end-systole was higher at the apex as compared to the base (-19.1±2.7 % at the apex, -19±2.9 % at the mid-ventricular slice, and -15.2±2.8 % at the base), while peak longitudinal strain was on average higher at the base (-14.7±3.4 % at the apex, -14.9±2.5 % at the mid-ventricular slice, and -15.7±2.8 % at the base) (Fig. 1a&d). On average, peak aortic outflow occurred at around 20% into the cardiac cycle when about 30% of torsion and about 50% of circumferential strain had been completed. **Diastole.** Early diastolic filling is initiated by LV untwist and strain relaxation, until peak mitral inflow velocity (-31.1±2.4 cm/s) is achieved (Fig. 1e&f). On average, peak mitral inflow occurred at around 70% into the cardiac cycle when about 45% of untwist and 65% of circumferential expansion had been completed. We hypothesize that late diastolic filling during atrial kick involves considerable untwisting to achieve complete relaxation. **Statistics.** Good intra-subject reproducibility was observed for all strain-based biomarkers (CCC in the range of 0.73-0.95), peak mitral inflow velocity (CCC=0.75), and for  $T_{ps-pm}$  (CCC=0.91) (Table 1). Inter-subject variability was higher for strain-rate biomarkers (Table 2). Power analysis calculations revealed that sample size of <25 are required to achieve 80% power for a 20% change in the least reproducible of the evaluated functional biomarkers (Table 2).

**Conclusion:** In conclusion, we have characterized cardiac function in NHPs using MR imaging.